Assessment of calculation methods for efficiency of straight fins of rectangular profile

L. J. Huang and R. K. Shah
Harrison Division, General Motors Corporation, Lockport, New York, USA

Fin efficiency evaluation of plate-fin surfaces in compact heat exchangers is done based on the idealizations of one-dimensional analysis, uniform thickness thin fins, uniform fin thermal conductivity, uniform heat transfer coefficients, uniform temperature ambient, and no temperature depression at the fin base. A critical assessment of these idealizations is presented. Whenever possible, additional quantitative new results are obtained to account for some of these effects. Relaxation of these idealizations will lower the value of ideal one-dimensional fin efficiency, but will have a relatively small effect, if the fin efficiency is above about 80 percent, based on the assessment in the paper. Some specific design recommendations are made for the determination of the fin efficiency for plate-fin heat exchangers.

Keywords: fin efficiency; straight fin; compact heat exchanger

Introduction

Fins are primarily used to increase the surface area and consequently to enhance the total heat transfer rate. Both conduction through the fin cross section and convection from the surface area take place. Hence, the surface temperature is generally lower than the base (prime surface) temperature if the fin convects heat to the fluid. This, in turn, reduces the temperature potential between the fin and the fluid for convection heat transfer, and the fin transfers less heat than if it had been at the base temperature. This is accounted for by the fin temperature effectiveness or fin efficiency η_f. The fin temperature effectiveness is defined as the ratio of the actual heat transfer through the fin to that which would be obtained if the entire fin were at the base temperature (i.e., the thermal conductivity of the fin material were infinite).

The fin efficiency for plate-fin surfaces in heat exchanger design is determined under the following idealizations (Gardner 1945, Kern and Kraus 1972, Kraus 1982, Mikhailov and Özişik 1984).

(1) The heat flow through the fin is steady state so that the temperature, t, in the fin does not vary with time.
(2) The contact thermal resistance between the fin and the base is negligible.
(3) There are no heat sources and sinks in the fin.
(4) Radiation heat transfer from the fin is neglected.
(5) The fin is so thin that its temperature, t, does not vary significantly over its thickness, δ_f.
(6) The thermal conductivity of the fin material is uniform and constant.
(7) The heat transfer coefficient for the fin surface, h, is uniform over the surface and constant with time.
(8) The temperature of the ambient fluid is uniform and constant.
(9) The temperature depression at the fin base is negligible in an extended surface heat exchanger.
(10) Longitudinal heat conduction in the fin along the fluid flow direction is negligible.

Idealizations 1–3 are common for the derivation of ideal one-dimensional (1-D) fin efficiency η_i for any fin geometry. Idealization 4 restricts the application of η_i to close fin spacings or relatively low temperature applications. Idealizations 5–10 have questionable validity. Ghai (1951) was apparently the first to discuss these latter idealizations qualitatively, and this was followed in short order also qualitatively by Gardner (1951) (in a discussion of Ghai's work), Fortescue (1957), and Hughes and Slack (1958).

In this paper, the ideal 1-D fin efficiency is first discussed. Then, a critical assessment of the limitations of idealizations 5–10 is presented. The relaxation on idealization 10 is discussed in the section of Fins with ambient fluid having nonuniform temperature (idealization 8). Whenever possible, additional quantitative new results are obtained to account for some of these effects, and specific design recommendations are made for the determination of the fin efficiency for "corrugated" fins used in plate-fin heat exchangers. Discussion is primarily restricted to straight fins of rectangular profile shown in Figure 1, but many of the conclusions are applicable to other fin geometries used in heat exchangers.

Ideal one-dimensional fin efficiency

Based on the aforementioned idealizations, the governing equations for straight fins of rectangular profile are as follows (Kraus 1982, Mikhailov 1984):

$$(d^2T/dY^2) - (mH)^2T = 0 \qquad (1)$$

Address reprint requests to Dr. Shah at the Harrison Division, General Motors Corporation, Lockport, NY 14094, USA.

Received 13 October 1991; accepted 13 January 1992

$$T_{Y=0} = 1 \tag{2}$$

$$(dT/dY)_{Y=1} = -K\mathrm{Bi}^* T \tag{3}$$

where, Y has been normalized by the fin height H, dimensionless fin temperature $T = (t - t_{a,1})/(t_0 - t_{a,1})$, the fin parameter $m = (hP/A_k k_f)^{1/2}$, the perimeter for surface convection $P = 2(L + \delta_f)$ in Figure 1, cross-section area for heat conduction $A_k = L\,\delta_f$ in Figure 1, $K = 2H/\delta_f$, and the Biot number at the fin tip $\mathrm{Bi}^* = h_e\,\delta_f/2k_f$, t_0 and $t_{a,1}$ are dimensional fin base and inlet ambient temperatures, and h and h_e are heat transfer coefficients of the fin surface and fin tip. Note that for $L \gg \delta_f$, $m = (2h/\delta_f k_f)^{1/2}$.

In the context of fin heat transfer, the Biot number, Bi, is the ratio of conduction resistance within the fin $[1/(2k_f/\delta_f)]$ to convection resistance at the fin surface $[1/h]$. A small value of Bi indicates the conduction resistance is small compared with the convection resistance; therefore, the temperature gradient within the fin is small compared with that at the fin surface, and indicates the fin may be approximated as thin for the fin efficiency calculation. A large value of Bi, however, indicates the conduction resistance is comparable to the convection resistance; therefore, the temperature gradient within the fin may not be negligible for the fin efficiency calculation (two-dimensional [2-D] approximation). Hence, Bi appears explicitly in the 2-D solution. The aforementioned idealization 5 may be written as $\mathrm{Bi} \ll 1$.

Equations 1–3 can be solved in a closed form (Kraus 1982, Mikhailov 1984), and the fin efficiency expressions for three boundary conditions are as follows.

Notation

A_f The surface area of the fins surface, m^2
A_p The surface area of the primary surface, m^2
Bi Biot number at the fin surface, $h\,\delta_f/2k_f$, dimensionless
Bi* Biot number at the fin tip, $h_e\,\delta_f/2k_f$, dimensionless
Bi^+ Modified Biot number defined in Equation 20, dimensionless
Bi_w Biot number based on the wall thermal conductivity, $h\,\delta_f/2k_w$, dimensionless
c_p Specific heat of ambient fluid, J/kg K
h Convective heat transfer coefficient on the fin surface, W/m^2 K
h_e Convective heat transfer coefficient at the fin tip, W/m^2 K
h_m Mean convective heat transfer coefficient on the fin surface with respect to the length, W/m^2 K
h_w Convective heat transfer coefficient on a wall (primary surface), W/m^2 K
H Fin height, m
I Modified Bessel function of first kind
k_f Fin thermal conductivity, W/m K
$k_{f,0}$ Fin thermal conductivity evaluated at the fin base temperature, W/m K
$k_{f,a}$ Fin thermal conductivity evaluated at the ambient fluid temperature at $X = 0$, W/m K
k_w Wall thermal conductivity, W/m K
K Fin aspect ratio, $2H/\delta_f$, dimensionless
L Fin length in the fluid flow direction, m
m Fin parameter, $(2h/k_f\,\delta_f)^{1/2}$, m^{-1}
m_y Modified fin parameter, defined in Equation 29, m^{-1}
q_0 Heat flux at the fin base, W
Q_0 Heat transfer rate at the fin base, $q_0\,\delta_f/k_f(t_0 - t_{a,1})$, defined in Equation 19, dimensionless
q_1 Heat transfer rate through the complete (extended surface) assembly, defined in Equation 50, W
r_k k_f/k_w, dimensionless
t Fin temperature, °C
t_0 Fin base temperature, °C
t_a Ambient fluid temperature, °C
$t_{a,1}$ Ambient fluid inlet temperature, °C
t_s The temperature of exposed wall surface in absence of the fin, °C
t_w The temperature of the fluid flow at the unfinned (the other fluid) side, °C
T Fin temperature, $(t - t_{a,1})/(t_0 - t_{a,1})$, dimensionless
$\bar{T}$ Mean fin temperature, $\int_0^1 T\,dZ$, dimensionless
T_a Ambient fluid temperature, $(t_a - t_{a,1})/(t_0 - t_{a,1})$, dimensionless
$T_{a,m}$ Mean ambient fluid temperature, dimensionless
u_a Mean velocity of ambient fluid, m/s
x Cartesian coordinate along the fluid flow direction, m
X x/L, dimensionless
y Cartesian coordinate along the fin height direction, m
Y y/H, dimensionless
z Cartesian coordinate along the fin thickness direction, m
Z $2z/\delta_f$, dimensionless

Greek symbols

α Thermal diffusivity, m^2/s
β A slope, defined by Equation 22, K^{-1}
Γ Gamma function
δ_f Fin thickness, m
δ_s Half fin spacing, as shown in Figure 1, m
δ_w Wall thickness, m
ε Normal total emissivity of a surface, dimensionless
ε_h $(\eta_i - \eta_f)/\eta_f$, Tables 4 and 6, dimensionless
ε_i $(\eta_i - \eta_f)/\eta_f$, Table 1, dimensionless
ε_k $(\eta_i - \eta_f)/\eta_f$, Table 3, dimensionless
ε_m $(\eta_{f,1} - \eta_f)/\eta_f$, Table 2, dimensionless
η_f Fin efficiency, dimensionless
$\eta_{f,1}$ Modified one-dimensional fin efficiency of Equation 21, dimensionless
η_i Ideal one-dimensional fin efficiency, dimensionless
θ_d $(t_0 - t_a)/(t_s - t_a)$, Table 8, dimensionless
κ A parameter, defined in Equation 24, dimensionless
ϕ Denotes a function
λ_m Eigenvalue of Equation 15
ρ Ambient fluid density, kg/m^3

Subscripts

a Ambient
b Bottom surface
e Fin tip
f Fin
i Ideal
m Mean
s Spacing
t Top surface
w Wall
0 $Y = 0$
1 $X = 0$

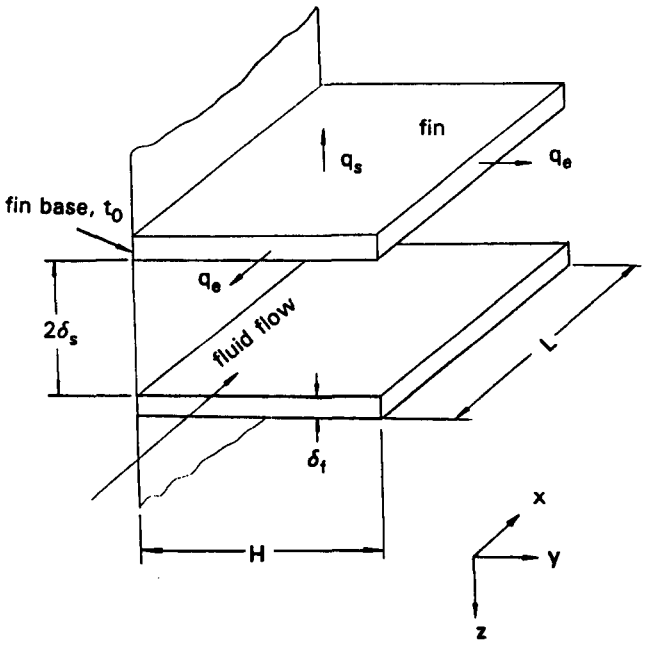

Figure 1 Nomenclature for the fin and ambient under consideration

For the fin with finite heat leakage at the fin tip (Bi* finite)

$$\eta_i = \frac{m^2H^2\tanh(mH) + mHK\mathrm{Bi}^*}{(K\mathrm{Bi}^* + m^2H^2)[mH + K\mathrm{Bi}^*\tanh(mH)]} \tag{4}$$

For the thin fin with an adiabatic fin tip (Bi* = 0)

$$\eta_i = \frac{\tanh(mH)}{mH} \tag{5}$$

For the very long thin fin with the fin tip temperature approaching the ambient temperature ($mH \gg 1$ and $mH \gg K\mathrm{Bi}^*$)

$$\eta_i = \frac{1}{mH} \tag{6}$$

For reference, the values of η_i of Equations 4–6 are related as follows: η_i of Equation 4 < η_i of Equation 5 < η_i of Equation 6. The fin efficiency η_i of Equation 4 will be within 5 percent of η_i of Equation 5 for $mH \leqslant 1$ and $\mathrm{Bi}^* \leqslant 0.01$. The fin efficiency η_i of Equation 5 will be within 5 percent of η_i of Equation 6 for $mH \geqslant 1.84$.

For most plate-fin heat exchangers, Equation 5 is used to determine the fin efficiency. The objective of this paper is to determine how accurate is the η_f prediction by Equation 5 in light of relaxing idealizations 5–10 as previously mentioned.

If the ambient fluid temperature is uniform only in the y–z plane and variable in the x direction (fluid flow direction) and longitudinal heat conduction within the fin along the x direction is neglected, Equations 1–3 may be modified as follows:

$$(\partial^2T/\partial Y^2) - (mH)^2(T - T_a) = 0 \tag{7}$$

$$T_{Y=0} = 1 \tag{2}$$

$$(\partial T/\partial Y)_{Y=1} = -K\mathrm{Bi}^*(T - T_a) \tag{8}$$

where the dimensionless ambient fluid temperature $T_a = (t_a - t_{a,1})/(t_0 - t_{a,1})$. Similar to Equations 1–3, the problem can be solved analytically and the solutions are the same as Equations 4–6. This is an expected result since Equations 4–6 are valid as long as the ambient fluid temperature is uniform locally at a given x.

Two-dimensional (thick) fin analysis

In this section, the literature is assessed to relax the thin fin idealization 5.

Avrami and Little (1942) analyzed the thin fin (2-D fin with the temperature varying in the y- and z-directions) problem for a straight fin of rectangular profile with finite end leakage. They solved the problem by using the method of separation of variables and provided the formula for heat transfer rate through the fin in an infinite series form. Keller and Somers (1959) applied the same method for an annular fin of constant thickness with finite end leakage and also provided the similar formula for heat transfer rate through the fin in an infinite series form. Unfortunately, Avrami and Little (1942) and Keller and Somers (1959) did not use the Biot number explicitly as an independent parameter. They reached conclusions for the validity of 1-D and 2-D solutions applicable only for small Biot numbers.

Irey (1968) used the Biot number as an independent parameter to analyze a circular pin fin in 2-D. He solved the problem by using the method of separation of variables and showed that the pin fins can be analyzed accurately (within 2 percent) using the ideal 1-D fin efficiency expression for Biot number Bi < 0.1. Lau and Tan (1973) extended Irey's solution to analyze a straight fin of rectangular profile and an annular fin, assuming the temperature of the ambient fluid as uniform. The differential equations governing a straight fin of rectangular profile are given by them as

$$(\partial^2T/\partial Y^2) + K^2(\partial^2T/\partial Z^2) = 0 \tag{9}$$

$$T_{Y=0} = 1, \qquad \text{for } 0 \leqslant Z \leqslant 1 \tag{10}$$

$$(\partial T/\partial Y)_{Y=1} = -K\mathrm{Bi}^*T_{Y=1}, \qquad \text{for } 0 \leqslant Z \leqslant 1 \tag{11}$$

$$(\partial T/\partial Z)_{Z=0} = 0, \qquad \text{for } 0 \leqslant Y \leqslant 1 \tag{12}$$

$$(\partial T/\partial Z)_{Z=1} = -\mathrm{Bi}T_{Z=1}, \qquad \text{for } 0 \leqslant Y \leqslant 1 \tag{13}$$

where dimensionless $Z = z/(\delta_f/2)$. Lau and Tan (1973) solved this problem by using the method of separation of variables and provided the formula for heat transfer rate through the fin in the form of an infinite series from which the following η_f expression has been derived by the present authors:

$$\eta_f = \frac{2}{(K\mathrm{Bi} + \mathrm{Bi}^*)}\sum_{m=1}^{\infty}\frac{\sin^2(\lambda_m)}{\lambda_m + \sin(\lambda_m)\cos(\lambda_m)} \times \frac{\mathrm{Bi}^*\cosh(\lambda_mK) + \lambda_m\sinh(\lambda_mK)}{\mathrm{Bi}^*\sinh(\lambda_mK) + \lambda_m\cosh(\lambda_mK)} \tag{14}$$

where

$$\lambda_m\tan\lambda_m - \mathrm{Bi} = 0, \qquad \mathrm{Bi} = (h\,\delta_f)/(2k_f) \tag{15}$$

Equation 14 indicates that $\eta_f = \phi(\mathrm{Bi}, K)$ when Bi* = 0 for 2-D geometries. In contrast, from Equation 5, the 1-D fin efficiency $\eta_i = \phi(mH)$ for Bi* = 0. Note that $mH = K\mathrm{Bi}^{1/2}$. Lau and Tan (1973) compared the fin efficiencies of Equations 14 and 5, and concluded that the major parameter governing the accuracy of the ideal 1-D fin efficiency is the Biot number, Bi. A comparison of Equations 5 and 14 is made in Table 1 with the relative error, $\varepsilon_i = (\eta_i - \eta_f)/\eta_f$. For solving Equation 14, 100 terms of the series were used to get 5-digit accuracy. Note that for most plate-fin heat exchangers, Bi ≪ 1 since $h \leqslant 500$ (W/m² K), $\delta_f \leqslant 0.25$ mm, and $k_f \approx 200$ (W/m K) for Al and 400 (W/m K) for Cu. Hence, the tabular results are provided for Bi ⩽ 1 in Table 1. Note that the results presented in Tables 1–6 are too close to illustrate graphically.

A review of Table 1 shows that for Bi ⩽ 0.01 and $K < 100$, the thin fin approximation (idealization 5) of Equation 5 introduces a maximum of 0.3 percent error.

Table 1 The fin efficiencies calculated by Equations 14 and 5 and the relative error ε_i percent of η_i with respect to η_f for Bi* = 0

Bi	K	η_f from Equation 14	η_i from Equation 5	ε_i percent
10^{-5}	1	1.000	1.000	*
10^{-5}	5	1.000	1.000	*
10^{-5}	10	1.000	1.000	*
10^{-5}	50	0.992	0.992	*
10^{-5}	100	0.968	0.968	*
10^{-4}	1	1.000	1.000	*
10^{-4}	5	0.999	0.999	*
10^{-4}	10	0.997	0.997	*
10^{-4}	50	0.924	0.924	*
10^{-4}	100	0.762	0.762	*
10^{-3}	1	0.999	1.000	0.026
10^{-3}	5	0.991	0.992	0.032
10^{-3}	10	0.968	0.968	0.031
10^{-3}	50	0.581	0.581	0.021
10^{-3}	100	0.315	0.315	0.017
10^{-2}	1	0.994	0.997	0.255
10^{-2}	5	0.922	0.924	0.292
10^{-2}	10	0.760	0.762	0.249
10^{-2}	50	0.200	0.200	0.159
10^{-2}	100	0.100	0.100	0.159
10^{-1}	1	0.945	0.968	2.454
10^{-1}	5	0.570	0.581	1.876
10^{-1}	10	0.311	0.315	1.480
10^{-1}	50	0.062	0.063	1.441
10^{-1}	100	0.031	0.032	1.441
1.0	1	0.645	0.762	18.042
1.0	5	0.181	0.200	10.792
1.0	10	0.090	0.100	10.764
1.0	50	0.018	0.020	10.764
1.0	100	0.009	0.010	10.764

* ε_i percent < 0.01 percent

Aparecido and Cotta (1990) modified the 1-D fin solution and extended it to cover the thick straight fin of rectangular profile and large values of Biot number. They have approximately taken into account the 2-D temperature distribution across the fin cross section by using the coupled integral equation approach. By integrating Equations 9–11 with respect to Z and using boundary conditions of Equations 12 and 13, Equations 9–11 become

$$(d^2\bar{T}/dY^2) - [\mathrm{Bi}/(1 + \mathrm{Bi}/4)]K^2\bar{T} = 0 \tag{16}$$

$$\bar{T}_{Y=0} = 1 \tag{17}$$

$$(d\bar{T}/dY)_{Y=1} = -K\mathrm{Bi}^*\bar{T} \tag{18}$$

where $\bar{T} = \int_0^1 T\,dZ$. This modified 1-D fin solution has been presented in terms of dimensionless heat transfer rate Q_0 at the fin base ($Y = 0$), which is defined as $Q_0 = q_0\,\delta_f/k_f(t_0 - t_{a,1})$, where q_0 is the heat flux at the fin base.

$$Q_0 = 2(\mathrm{Bi}^+)^{1/2} \times \frac{\mathrm{Bi}^* \cosh[K(\mathrm{Bi}^+)^{1/2}] + (\mathrm{Bi}^+)^{1/2} \sinh[K(\mathrm{Bi}^+)^{1/2}]}{\mathrm{Bi}^* \sinh[K(\mathrm{Bi}^+)^{1/2}] + (\mathrm{Bi}^+)^{1/2} \cosh[K(\mathrm{Bi}^+)^{1/2}]} \tag{19}$$

where

$$\mathrm{Bi}^+ = \frac{\mathrm{Bi}}{1 + \mathrm{Bi}/4} \tag{20}$$

The fin efficiency may be easily obtained by using the relation

$$\eta_f = \frac{Q_0}{2K\mathrm{Bi} + 2\mathrm{Bi}^*} \tag{21}$$

Note that Equation 21 relating η_f to Q_0 is derived from the basic definition of η_f, and hence is valid for 1-D, 2-D solutions, or any modifications. The relative error ε_m percent of Equation 21 with respect to exact 2-D solution of Equation 14 is listed in Table 2 for Bi* = 0.

A review of the results of Table 2 reveals that for Bi < 0.01 and K < 100, the modified 1-D solution of Equation 21 introduces a maximum error of 0.06 percent. Equations 21 and 19 are easily employed for the evaluation of η_f compared with Equation 14, which requires the determination of eigenvalues in addition to solving the infinite series expression.

Fins with nonuniform thermal conductivity

In this section, the work is reported on the fins with nonuniform thermal conductivity to relax the idealization 6.

Hung and Appl (1967) analyzed the efficiency of a straight fin of rectangular profile by considering the thermal conductivity as a function of the temperature. The analysis used a bounding procedure (the steepest descent method) that yielded analytical and continuous bounding functions for the temperature distribution. The thermal conductivity was assumed to be linearly varying, with the temperature excess over the ambient. The fin temperature was presented in tabular

Table 2 The fin efficiencies calculated by Equations 14 and 21 and the relative error ε_m percent of Equation 21 with respect to Equation 14 for Bi* = 0

Bi	K	η_f from Equation 14	$\eta_{f,1}$ from Equation 21	ε_m percent
10^{-5}	1	1.000	1.000	*
10^{-5}	5	1.000	1.000	*
10^{-5}	10	1.000	1.000	*
10^{-5}	50	0.992	0.992	*
10^{-5}	100	0.968	0.968	*
10^{-4}	1	1.000	1.000	*
10^{-4}	5	0.999	0.999	*
10^{-4}	10	0.997	0.997	*
10^{-4}	50	0.924	0.924	*
10^{-4}	100	0.762	0.762	*
10^{-3}	1	0.999	1.000	*
10^{-3}	5	0.991	0.991	*
10^{-3}	10	0.968	0.968	*
10^{-3}	50	0.581	0.581	*
10^{-3}	100	0.315	0.315	*
10^{-2}	1	0.994	0.994	*
10^{-2}	5	0.922	0.922	0.061
10^{-2}	10	0.760	0.760	0.055
10^{-2}	50	0.200	0.200	0.034
10^{-2}	100	0.100	0.100	0.034
10^{-1}	1	0.945	0.945	0.033
10^{-1}	5	0.570	0.570	0.289
10^{-1}	10	0.311	0.311	0.206
10^{-1}	50	0.062	0.062	0.196
10^{-1}	100	0.031	0.031	0.196
1.0	1	0.645	0.638	−1.077
1.0	5	0.181	0.179	−0.921
1.0	10	0.090	0.089	−0.930
1.0	50	0.018	0.018	−0.930
1.0	100	0.009	0.009	−0.930

* ε_n percent < 0.01 percent

and graphical form with the effects of heat generation, a linear variation of heat transfer coefficient, finite radiation, and linearly varying thermal conductivity. Our calculations indicate that when the fin efficiency is 80 percent and the ratio of thermal conductivity at the fin base to that at the fin tip is 1.1, the fin efficiency predicted by Equation 5 is about 1.7 percent lower when there is no heat generation and a constant heat transfer coefficient. Thus, the influence of moderately linear thermal conductivity of the fin has a negligible influence on η_i for $\eta_i > 80$ percent.

Aziz and Enamul Huq (1975) and Aziz (1977) solved the same problem using a perturbation method. They assumed that the thermal conductivity varies linearly with the temperature

$$k_f = k_{f,a}[1 + \beta(t - t_a)] \tag{22}$$

where $k_{f,a}$ is the fin thermal conductivity at the ambient fluid temperature and β is a constant. The fin efficiency was presented as a function of κ, as follows, considering no heat generation:

$$\eta_f = \tanh(mH)/mH + \kappa \tanh^3(mH)/(3mH) \tag{23}$$

where

$$\kappa = (k_{f,0} - k_{f,a})/k_{f,a} = \beta(t_0 - t_a) \tag{24}$$

Here, $k_{f,0}$ is the thermal conductivity at the fin base. A comparison of Equation 23 with Equation 5 is made in Table 3 with the relative error, ε_k, computed as $(\eta_i - \eta_f)/\eta_f$.

A review of the results of Table 3 reveals that η_i of Equation 5 underpredicts the fin efficiency up to about 1.7 percent for $\eta_i = 80$ percent for the variation of the thermal conductivity κ of 10 percent, when the fin is being cooled. For fins with most common metals, $\kappa \leqslant 10$ percent for temperature difference of about 200°C between $y = 0$ and H. Thus, for $\eta_i > 80$ percent and $\kappa < 10$ percent, the aforementioned specific variation of the thermal conductivity has a negligible effect on η_f. If the fin were being heated, just the opposite effect would have been found, i.e., the η_i computed by Equation 5 would have been slightly higher than the actual fin efficiency when accounting for the linear variation in the thermal conductivity with the temperature.

A rectangular composite fin was investigated by Barrow (1985) to study the effects of frosting on the heat transfer performance of a finned evaporator surface of a heat pump. In that study, it was found that the effect of a uniformly thick layer of low conductivity frost on the overall heat transfer rate was small even when the thickness of the frost was many times that of the fin itself. The loss of heat transfer performance was attributed to the reduction in the flow rate as a result of an increase of the external flow resistance associated with the increased blockage caused by the frost, rather than the insulation effect of the layer. These findings by Barrow (1985) were based on a "parallel resistance" model for the fin heat flow originally used by Schenck (1960) and adopted by Epstein and Sandhu (1978). A more accurate analysis is presented by Barrow *et al.* (1986). In their work, the finite difference, finite element, and exact mathematical methods were used with special reference to the 2-D effects on heat transfer from the fin. In particular, a high conductivity rectangular profile fin with a uniformly thick low conductivity layer of specified dimensions and properties was studied with a view to quantifying these effects on the performance of frosted or fouled heat exchangers. They concluded that the high conductivity fin plays a dominant role in the heat transfer mechanism, with the reduction of heat flow by the so-called "insulating layer" due to frosting being surprisingly small. However, our recalculations using the equations of Barrow *et al.* (1986) indicate that the reduction of heat transfer due to frosting, which is confined principally to the low conductivity layer, is not insignificant; it is about 8 percent at typical η_f values of 96 percent.

Table 3 The fin efficiencies calculated by Equations 5 and 23 and the relative error ε_k percent of Equation 5 with respect to Equation 23

κ percent	η_i	η_f	ε_k percent
5	0.900	0.904	0.453
5	0.800	0.807	0.840
5	0.700	0.708	1.144
5	0.600	0.608	1.383
5	0.500	0.508	1.530
10	0.900	0.908	0.916
10	0.800	0.814	1.680
10	0.700	0.716	2.288
10	0.600	0.616	2.766
10	0.500	0.516	3.060

Fins with variable heat transfer coefficients

Influence of nonuniform heat transfer coefficient over the fin surface on the fin efficiency (relaxation of idealization 7) is considered in this section.

Ghai and Jakob (1950) and Ghai (1951) have experimentally demonstrated that heat transfer coefficients attained significantly greater values at the fin tip than at the fin base and concluded that the idealization of uniform heat transfer coefficient is not necessarily realistic. Significant variations in the heat transfer coefficient have also been demonstrated by Harris and Wilson (1961), Stachiewicz and McKay (1963), Stynes and Myers (1964). Saboya and Sparrow (1976) show that the heat transfer coefficient can vary by a factor of 50 (and not 50 percent) over a flat plain fin in a one-tube-row finned exchanger. Transient techniques using model fin tubes injected into a hot airstream were used by Jones and Russell (1978, 1980) to measure local heat transfer coefficients. A large variation was also found.

Han and Lefkowitz (1960) assumed a power-law variation of h over the fin height, H. They considered the heat transfer coefficient increasing with y in the following form:

$$h(Y) = h_m(1 + \gamma)(Y)^{\gamma} \tag{25}$$

where h_m is the average heat transfer coefficient and γ is a constant. After a rather involved transformation of variables, Han and Lefkowitz showed that with the boundary conditions of the constant fin base temperature, t_0, and an insulated tip, the fin efficiency is given by

$$\eta_f = [(\gamma + 2)^{\gamma}(\gamma + 1)/(mH)^{2(\gamma+1)}]^{1/(\gamma+1)}AB \tag{26}$$

where

$$A = I_{(\gamma+1/\gamma+2)}(m_\gamma H)/I_{-(\gamma+2/\gamma+1)}(m_\gamma H) \tag{27}$$

$$B = \Gamma(\gamma + 1/\gamma + 2)/\Gamma(1/\gamma + 2) \tag{28}$$

$$m_\gamma = 2(\gamma + 1)^{1/2}m/(\gamma + 2) \tag{29}$$

It was concluded that the idealization of uniform heat transfer coefficient may lead to gross errors in analyzing heat transfer of extended surfaces. For a particular linear variation ($y = 1$), the fin efficiency of Equation 26 may be simplified as

$$\eta_f = \frac{6\Gamma(2/3)I_{2/3}(m_1H)}{\Gamma(1/3)(mH)^4 I_{-2/3}(m_1H)} \tag{30}$$

The fin efficiencies of Equation 5 and 30 and the relative error of Equation 5 with respect to Equation 30 are presented in Table 4, where the relative error $\varepsilon_h = (\eta_i - \eta_f)/\eta_f$.

A comparison of Equations 30 and 5 in Table 4 reveals that η_f of Equation 30 is lower by 6, 17, and 24 percent for η_i of Equation 5 of 90, 80, and 70 percent, respectively, although

Table 4 The fin efficiencies of Equations 5 and 30 and the relative error ε_h of Equation 5 with respect to Equation 30

mH	η_f	η_i	ε_h percent
0.1	0.993	0.997	0.33
0.2	0.974	0.987	1.31
0.3	0.944	0.971	2.86
0.4	0.905	0.950	4.91
0.5	0.861	0.924	7.34
0.6	0.814	0.895	10.02
0.7	0.765	0.863	12.85
0.8	0.717	0.830	15.72
0.9	0.672	0.796	18.53
1.0	0.628	0.762	21.22
1.1	0.588	0.728	23.74
1.2	0.551	0.695	26.06
1.3	0.517	0.663	28.16
1.4	0.486	0.632	30.03
1.5	0.458	0.603	31.69
1.6	0.433	0.576	33.13
1.7	0.409	0.550	34.39
1.8	0.388	0.526	35.47
1.9	0.369	0.503	36.39
2.0	0.351	0.482	37.18
3.0	0.236	0.332	40.52
4.0	0.177	0.259	40.86
5.0	0.142	0.200	40.67
6.0	0.119	0.167	40.36
7.0	0.102	0.143	39.97
8.0	0.090	0.125	39.53
9.0	0.080	0.111	39.02
10.0	0.072	0.100	38.46

the mean value of the nonuniform heat transfer coefficient h_m is equal to the value of the uniform case. These results (and Table 4) clearly indicate that any significant variability in the heat transfer coefficient over the fin surface will reduce the actual fin efficiency significantly. Since h is determined experimentally for most heat exchanger surfaces by using Equation 5 in the original data reduction, the subsequent use of Equation 5 for the design of a heat exchanger should not introduce the large errors shown by Table 4. However, one needs to be aware of the impact of nonuniform h on η_f, particularly, if there are significant differences in η_f between the original data and that of the actual heat exchangers.

Chen and Zyskowski (1963) analyzed the problem with an exponential variation of h versus y by using the same solution procedure as that in Han and Lefkowitz (1960). Their conclusion is similar to that of Han and Lefkowitz (1960). Cumo *et al.* (1965) conducted a 2-D study with a more general form of the variation of the heat transfer coefficient; the fin efficiency was obtained numerically. With a few numerical results, they again demonstrated the conclusions of the Han and Lefkowitz (1960) and Chen and Zyskowski (1963). Snider and Kraus (1982) demonstrated how perturbation theory could be used to estimate the effect of an arbitrary variation in the heat transfer coefficient. However, no specific results are presented.

Ünal (1985, 1987) analyzed 1-D straight fin of rectangular profile assuming that the heat transfer coefficient is a power function of the difference between the temperature of the fin and that of the ambient fluid. He considered the heat transfer coefficient as a function of the dimensionless T in the following form:

$$h = aT^n \tag{31}$$

where a and n are positive constants. After a rather involved transformation of variables, Ünal (1985) showed that with the boundary conditions of the constant fin base temperature t_0 and an insulated tip, the fin temperature of Equation 1 has a closed-form solution for $n = 1$ and 2 as follows.

$$\zeta F(\phi/\alpha) = a_1^{1/2} Y \tag{32}$$

where

$$a_1 = (4aT_e^n H^2)/[(n+2)k_f \delta_f] \tag{33}$$

T_e is the fin tip temperature and may be evaluated by solving Equation 32, and $F(\phi/\alpha)$ is the Legendre's (incomplete) normal elliptic integral of the first kind. For $n = 1$

$$\zeta = 3^{-1/4} \tag{34}$$

$$\cos\phi = (3^{1/2} + 1 - T/T_e)/(3^{1/2} - 1 + T/T_e) \quad \text{for } 0 \leqslant \phi \leqslant \pi \tag{35}$$

$$\alpha = \pi/12 \tag{36}$$

For $n = 2$

$$\zeta = 2^{-1/2} \tag{37}$$

$$\cos\phi = T_e/T \quad \text{for } 0 \leqslant \phi \leqslant \pi \tag{38}$$

$$\alpha = \pi/4 \tag{39}$$

The fin efficiency is given as

$$\eta_f = \frac{2T_e^{n+1}(T_e^{-(n+2)} - 1)^{1/2}}{(n+2)a_1^{1/2}} \tag{40}$$

For $n = 1$ and 2, a of Equation 31 can be approximated as $(2h_m)/(1 + T_e)$ and $(3h_m)/(1 + T_e + T_e^2)$, respectively; therefore, a_1 and η_f of Equations 33 and 40 take the form shown in Table 5. Here, h_m is the mean heat transfer coefficient defined as the integrated average of local heat transfer coefficient with respect to the length. It should be noted that T_e is only a function of n and mH and may be evaluated by solving Equation 32 by setting $Y = 1$; therefore, for $n = 1$ and 2, η_f is only a function of mH. The fin efficiencies of Equations 5 and 40 and the relative error of Equation 5 with respect to Equation 40 are presented in Table 6 for $n = 1$ and 2, where the relative error $\varepsilon_h = (\eta_i - \eta_f)/\eta_f$.

A comparison of Equations 40 and 5 in Table 6 reveals that η_f of Equation 40 is higher by 1 percent when $n = 1$ and 2.4 percent when $n = 2$ for η_i of Equation 5 as 85 percent, although the mean value of the nonuniform heat transfer coefficient is equal to the value for the uniform case.

Barrow *et al.* (1986) investigated the effect of variable heat transfer coefficient of a composite fin on heat transfer. The problem was solved by finite difference, finite element, and exact mathematical analyses. In particular, a high conductivity rectangular-profile fin with a uniformly thick low-conductivity layer of specified dimensions and properties was studied with a view to quantifying these effects on the performance of frosted or fouled heat exchangers. The reduction of heat transfer due to (1) 2-D effects, which were confined principally to the layer, and (2) a linearly varying heat transfer coefficient was about

Table 5 Expressions for a_1 and η_f of Equations 33 and 40 for n = 1 and 2

	n = 1	n = 2
a_1	$\frac{4T_e}{3(1+T_e)}(mH)^2$	$\frac{3T_e^2}{2(1+T_e+T_e^2)}(mH)^2$
η_f	$\frac{T_e^{n+1/2}[(T_e^{-3}-1)(1+T_e)]^{1/2}}{3^{1/2}(mH)}$	$\frac{T_e^n(T_e^{-4}-1)(1+T_e+T_e^2)]^{1/2}}{6^{1/2}(mH)}$

Table 6 The fin efficiencies of Equations 5 and 40 and the relative error ε_h of Equation 5 with respect to Equation 40

		$n = 1$		$n = 2$	
mH	η_i	η_f	ε_h percent	η_f	ε_h percent
0.1	0.997	0.997	0.00	0.997	0.00
0.2	0.987	0.987	−0.01	0.987	−0.02
0.3	0.971	0.971	−0.04	0.972	−0.07
0.4	0.950	0.951	−0.11	0.952	−0.22
0.5	0.924	0.927	−0.26	0.929	−0.50
0.6	0.895	0.900	−0.49	0.904	−0.94
0.7	0.863	0.871	−0.84	0.877	−1.56
0.8	0.830	0.841	−1.29	0.850	−2.38
0.9	0.796	0.811	−1.86	0.824	−3.37
1.0	0.762	0.781	−2.53	0.798	−4.53
1.1	0.728	0.753	−3.30	0.773	−5.83
1.2	0.695	0.725	−4.15	0.749	−7.23
1.3	0.663	0.698	−5.05	0.726	−8.71
1.4	0.632	0.673	−6.00	0.705	−10.25
1.5	0.603	0.649	−6.98	0.684	−11.80
1.6	0.576	0.626	−7.98	0.665	−13.37
1.7	0.550	0.604	−8.97	0.647	−14.92
1.8	0.526	0.584	−9.96	0.630	−16.45
1.9	0.503	0.565	−10.94	0.613	−17.95
2.0	0.482	0.547	−11.89	0.598	−19.40
3.0	0.332	0.413	−19.67	0.482	−31.14
4.0	0.250	0.331	−24.61	0.408	−38.71
5.0	0.200	0.277	−27.86	0.356	−43.83
6.0	0.167	0.239	−30.15	0.318	−47.62
7.0	0.143	0.210	−31.89	0.290	−50.68
8.0	0.125	0.187	−33.28	0.266	−53.09
9.0	0.111	0.169	−34.43	0.242	−54.13
10.0	0.100	0.155	−35.42	0.219	−54.36

11 percent at typical η_f values of 96 percent, in contrast to 8 percent for a constant heat transfer coefficient mentioned earlier. This again indicates a significant effect on η_f.

For a horizontal fin (Figure 2) in a natural convection environment, the heat transfer coefficient attains significantly greater values on the fin top surface than that on the fin bottom surface (Özişik, 1985). Look (1988, 1989) presented the results of an investigation of these unequal convection coefficient effects on the heat loss from a straight fin of rectangular profile. He employed heat balance integral approaches originally used by Steir (1976) to the 2-D thick fin model with uniform ambient temperature. A comparison was made of heat transfer $Q^{=}$ by the fin where $\mathrm{Bi}_t = \mathrm{Bi}_b$ and the heat transfer $Q^{\neq}$ by the fin when $\mathrm{Bi}_t > \mathrm{Bi}_b$, where superscripts $=$ and $\neq$ denote the heat transfer coefficients on the top and bottom surfaces equal and unequal, respectively; and subscripts t and b denote the heat transfer coefficient on the top surface and bottom surface of the fin, respectively. He concluded that $Q^{=}/Q^{\neq}$ can be as much as 1.95 for $\mathrm{Bi}_b/\mathrm{Bi}_t = 0$, $\mathrm{Bi}_t = 0.01$, and $K = 5$. Note that Look (1988, 1989) computed $Q^{=}$ by assuming the Biot numbers on the top and bottom surfaces as equal to Bi_t, but not $(\mathrm{Bi}_t + \mathrm{Bi}_b)/2$. Based on our calculations, $1 < Q^{=}/Q^{\neq} < 1.05$ for $\mathrm{Bi}_b/\mathrm{Bi}_t = 0$–1, $\mathrm{Bi}_t \leqslant 0.01$, and $K = 5$–100. Here, we used equations of Look (1989) to calculate $Q^{\neq}$ and we used Bi $[= (\mathrm{Bi}_t + \mathrm{Bi}_b)/2]$ in Equation 14 to calculate η_f, and used this η_f in Equation 21 to obtain Q_0, which is equal to $Q^{=}$. Incidentally, the first column of Table 1 of Look (1989) should be $\mathrm{Bi}_b/\mathrm{Bi}_t$.

Recently, Ma *et al.* (1991) studied the effect of 2-D rectangular fin with variable heat transfer coefficients using a Fourier series approach. They assumed that the fin temperature is independent of x as shown in Figure 1. The dimensionless

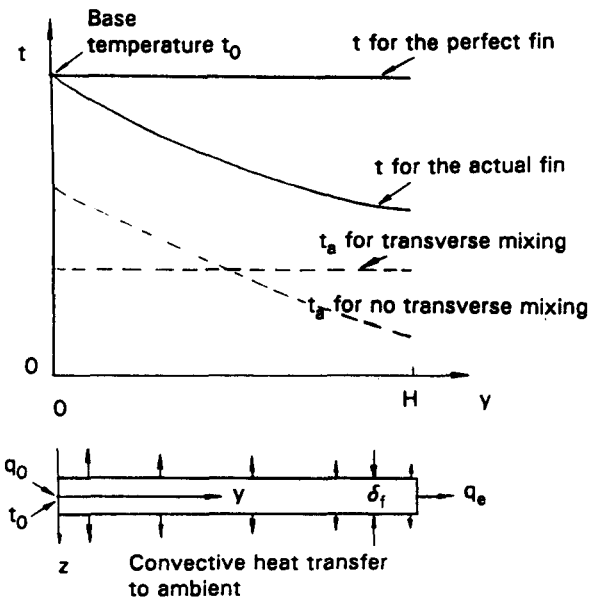

Figure 2 Temperature distributions for actual and perfect fin with and without transverse mixing ambient temperature

T of the fin was provided in a complicated infinite series integral. The variation of h on the fin surface was allowed to be arbitrary. However, they solved a three-dimensional fin problem using their 2-D analysis to demonstrate the combined effects of a thick fin and variable heat transfer coefficient with

the following data: fin height $H = 0.04$ m, the cross section of the square fin as 0.01×0.01 m, $k_f = 100$ W/m K, $h = 50$ W/m^2 K, $h = 50$ W/m^2 K on all surfaces along the first 0.01 m of fin height, $h = 100$ W/m^2 K on all surfaces along the remaining 0.03 m of fin height, and an adiabatic fin tip. The results were compared with the 1-D solution originally proposed by Shah (1971) and Kraus *et al.* (1978) and adopted by Snider and Kraus (1982). In this 1-D method, the whole fin is considered as two fins in cascade, and the average heat transfer coefficient is determined by use of a lengthwise weighting function. They concluded that the heat transfer computed by the 2-D analysis is 8.7 percent higher than that by 1-D solution for η_i of Equation 5 of 85 percent.

Fins with ambient fluid having nonuniform temperature

In this section, the idealization 8 of fins with uniform ambient fluid temperature is relaxed.

In 1-D analyses, it is assumed that the temperature distribution of the fluid flowing over the fin is uniform (i.e., fluid is perfectly mixed) at any cross section. In reality, however, this is not the case. The temperature of the ambient fluid varies exponentially at any flow cross section due to (1) a different temperature potential and different heat transfer rates along the coordinate y, and (2) no transverse mixing of the fluid as shown in Figure 2. Shah (1985) idealized the ambient temperature profile at any flow cross section parallel to the fin temperature profile; the difference $t - t_a$ between the fin and ambient temperature at any x was constant, independent of y; and the efficiency of a straight fin of rectangular profile with the insulated tip was

$$\eta_f = 1/[1 + (m^2H^2/3)] \tag{41}$$

Prediction of Equation 41 are 10, 4 and 1 percent lower than η_i of Equation 5 for $\eta_i = 50$, 65, and 80 percent, respectively. Thus, for $\eta_i > 80$ percent, the aforementioned specific variation in the temperature of the ambient fluid has a negligible effect on η_f.

Variable ambient fluid temperature in x–y coordinates

Since no generalized results are available to take into account actual variations in the ambient fluid flow (x) direction, this problem is solved here numerically considering the ambient fluid as air. However, the resultant fin efficiencies from the analysis should be valid for other ambient fluids. Note that in this case, the thin fin temperature will be considered 2-D, i.e., varying with y as well as x. Hence, longitudinal conduction in the thin fin (in the x direction) will be considered finite. The fin efficiency in this case depends on one additional parameter H/L in addition to mH and Bi*.

Consider that the mixing along the fin height H (transverse mixing) may be negligible after a short distance along the fin flow length L (Figure 1) as would be the case for laminar and low Reynolds number turbulent flow. In such a case, the ambient temperature is a function of x and y. The nomenclature for the fin to be analyzed is described in Figures 1 and 2. The fin is considered to be thin and the temperature, t, does not vary significantly over its thickness, δ_f. The temperature of the fin is considered to be 2-D in the x and y coordinates. The governing equations for the fin and ambient are as follows.

$$(H/L)^2(\partial^2T/\partial X^2) + (\partial^2T/\partial Y^2) - (mH)^2(T - T_a) = 0 \tag{42}$$

$$T_{Y=0} = 1, \quad \text{for } 0 \leqslant X \leqslant 1 \tag{43}$$

$$(\partial T/\partial Y)_{Y=1} = 0, \quad \text{for } 0 \leqslant X \leqslant 1 \tag{44}$$

$$(\partial T/\partial X)_{X=0} = 0, \quad \text{for } 0 \leqslant Y \leqslant 1 \tag{45}$$

$$(\partial T/\partial X)_{X=1} = 0, \quad \text{for } 0 \leqslant Y \leqslant 1 \tag{46}$$

where $X = x/L$; all other variables have been defined previously, or see the Notation. The governing equation for the ambient fluid is

$$(\partial T_a/\partial X) = [\mathrm{Nu}_L/(\mathrm{Re\ Pr})](T - T_a) \tag{47}$$

with the boundary condition as

$$T_a|_{X=0} = 0 \tag{48}$$

where Nusselt number $\mathrm{Nu}_L = hL/k_a$, Prandtl number $\mathrm{Pr} = \nu/\alpha$ and Pr = 0.7 for air, Reynolds number $\mathrm{Re} = \rho u_a \delta_s/\nu$, and k_a, ν, α, ρ, δ_s, u_a are the ambient fluid thermal conductivity, kinematic viscosity, thermal diffusivity, density, half-fin spacing, and the average velocity of the ambient fluid, respectively. Governing Equations 42–48 for the fin temperature, T, and ambient temperature, T_a, are solved simultaneously.

When the ambient fluid is idealized as mixed in the transverse direction, its temperature is 1-D and is only a function of X. In this case, Equation 42 is not valid, instead it is modified as

$$(H/L)^2(\partial^2T/\partial X^2) + (\partial^2T/\partial Y^2) - (mH)^2(T - T_{a,m}) = 0 \tag{49}$$

with the boundary conditions of Equations 43–46 still valid. The cross-sectional average ambient temperature, $T_{a,m}$ (which is only a function of X) of Equation 49 is obtained by averaging 2-D ambient temperature, T_a, where T_a is obtained by solving Equations 47 and 48.

Equations 42 and 49 were solved using a numerical procedure based on a central difference scheme having a second-order accuracy. The alternating direction implicit method was employed to solve the difference equations iteratively starting from appropriate guesses. This method is unconditionally stable (Anderson *et al.* 1984).

Results and discussions

The fin efficiencies for ambient fluid with no transverse mixing ($\eta_{f,2}$), with transverse ($\eta_{f,1}$), and the ideal 1-D case (η_i of Equation 5) are presented in Table 7 and the corresponding variations in T_a along X are shown in Figure 3 for various values of mH. The following specific values are used to generate the results: the ambient fluid is air with Pr = 0.7, Re = 10^4, fin base temperature $t_0 = 200$°C, and inlet ambient temperature $t_{a,1} = 30$°C.

In Figure 3, the local temperature of ambient fluid with no transverse mixing and with transverse mixing are plotted against the fluid flow direction for the case of low mH ($= 0.25$) and large mH ($= 1$). For the no transverse mixing case, the axial variation of the ambient fluid temperature is shown for two specific locations along the fin, $Y = 0$ and 1. When mH is low ($mH = 0.25$), the fin efficiency is high and the temperature variation along the fin is small. Therefore, the ambient fluid temperature variation along the Y-direction is small, as found by the curves for $Y = 0$ and 1 in Figure 3 being almost the same. Since the heat transfer to the ambient fluid is low due to a low value of h (low mH), the ambient fluid temperature rise along the X-direction (fluid flow direction) is small, about 30°C as compared with $(t_0 - t_{a,1}) = 170$°C. For a large value of mH ($mH = 1$), the fin efficiency is low, the fin temperature variation across the fin is large, the ambient fluid temperature variation along the Y-direction (between $Y = 0$ and 1) is large

Table 7 Effect with and without transverse mixing of ambient fluid on the fin efficiency for $H/L = 0.2$, 0.5, and 1.0

		$H/L = 0.2$		$H/L = 0.5$		$H/L = 1.0$	
mH	η_i	$\eta_{f,2}$	$\eta_{f,1}$	$\eta_{f,2}$	$\eta_{f,1}$	$\eta_{f,2}$	$\eta_{f,1}$
0.1	0.997	0.997	0.997	0.997	0.997	0.997	0.997
0.2	0.987	0.987	0.987	0.987	0.987	0.987	0.987
0.3	0.971	0.971	0.971	0.971	0.971	0.971	0.971
0.4	0.950	0.950	0.950	0.950	0.950	0.950	0.950
0.5	0.924	0.924	0.924	0.924	0.924	0.924	0.924
0.6	0.895	0.895	0.895	0.895	0.895	0.895	0.895
0.7	0.863	0.863	0.863	0.863	0.863	0.863	0.863
0.8	0.830	0.829	0.830	0.829	0.830	0.830	0.830
0.9	0.796	0.794	0.796	0.796	0.796	0.796	0.796
1.0	0.762	0.759	0.762	0.761	0.762	0.762	0.762
1.1	0.728	0.724	0.728	0.727	0.728	0.728	0.728
1.2	0.695	0.685	0.695	0.694	0.695	0.695	0.695
1.3	0.663	0.655	0.663	0.662	0.662	0.663	0.662
1.4	0.632	0.622	0.632	0.631	0.632	0.632	0.632
1.5	0.603	0.590	0.603	0.601	0.603	0.603	0.603
1.6	0.576	0.559	0.576	0.573	0.576	0.576	0.576
1.7	0.550	0.530	0.550	0.546	0.550	0.550	0.550
1.8	0.526	0.502	0.526	0.521	0.526	0.525	0.526
1.9	0.503	0.475	0.503	0.497	0.503	0.502	0.503
2.0	0.482	0.450	0.482	0.475	0.482	0.481	0.482
3.0	0.332	0.267	0.332	0.311	0.332	0.326	0.332
4.0	0.250	0.171	0.250	0.215	0.250	0.240	0.250
5.0	0.200	0.118	0.200	0.155	0.200	0.185	0.200
6.0	0.167	0.086	0.167	0.116	0.167	0.148	0.167
7.0	0.143	0.065	0.143	0.089	0.143	0.121	0.143
8.0	0.125	0.052	0.125	0.070	0.125	0.100	0.125
9.0	0.111	0.045	0.110	0.057	0.111	0.084	0.111
10.0	0.100	0.034	0.099	0.047	0.099	0.071	0.100

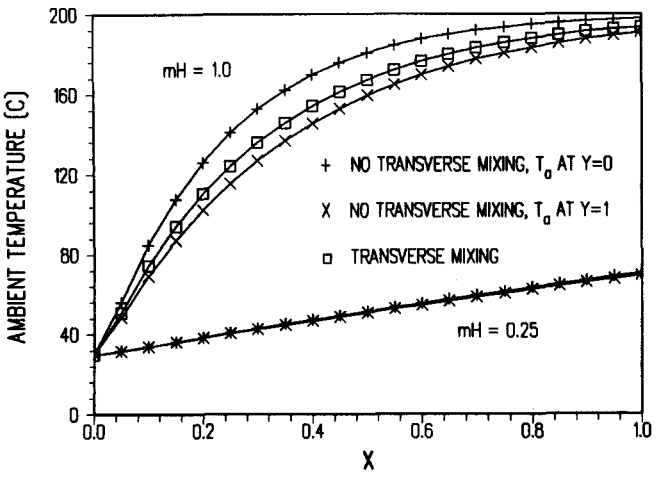

Figure 3 Local ambient temperature with and without transverse mixing effects

(about 20°C), and the heat transfer to the ambient is high due to high value of h (high mH). Therefore, the ambient fluid temperature rise along the X-direction is large, about 150°C as compared with $(t_0 - t_{a,1}) = 170$°C.

The effects of no transverse mixing of ambient fluid and transverse mixing of ambient fluid on the fin efficiency are listed for various values of mH in Table 7 for $H/L = 0.2$, 0.5, and 1.0. In Table 7, $\eta_{f,2}$ is the fin efficiency obtained by solving Equations 42–48 using no transverse mixing of the ambient fluid (a function of x and y), $\eta_{f,1}$ is the fin efficiency obtained by solving Equations 49 and 43–48 using transverse mixing of ambient fluid (a function of x only), and η_i is ideal fin efficiency of Equation 5. When mH is small, the temperature variation of the ambient fluid in the Y-direction for the no transverse mixing case is small, hence the fin efficiencies for the no transverse mixing and transverse mixing cases are almost the same. When mH is large, the temperature variation of the ambient fluid in the Y-direction for the no transverse mixing case is large (Figure 3), and the fin efficiency for the no transverse mixing case is lower than that of the transverse mixing case (Table 7). Thus, for $\eta_i > 60$ percent ($mH < 1.5$), this reduction is less than 1 percent. The results also depict two other features: (1) the fin efficiency $\eta_{f,1}$ of the transverse mixing case is almost the same as the ideal 1-D solution for $\eta_f \geq 10$ percent, the minor difference between the two cases is finite (for $\eta_{f,1}$) versus zero longitudinal conduction (for η_i) in the fin along the X-direction; and (2) as mH increases and H/L decreases, the effect of longitudinal heat conduction increases. However, again, the effect is negligible for $\eta_i > 80$ percent regardless of the values of H/L and mH considered.

Fins with temperature depression at the base

In an extended surface heat exchanger, when the fin area is an order of magnitude higher than the primary (exposed wall) surface area, a large amount of heat is transferred through the fins compared with that through the primary surface. As a result, the fin base temperature is lower than the primary surface temperature, if the fin is being cooled. This difference is referred to as the fin base temperature depression. This, in turn, may affect the heat transfer through the fin, and, effectively, results in reduced or increased fin efficiency for the same base

temperature. In this section, the literature is assessed on this effect to relax the idealization 9.

Sparrow and Hennecke (1970) were the first investigators to analyze the extent of temperature depression at the fin base in detail. They numerically evaluated the case of a single straight fin of rectangular profile affixed to a thick wall of large surface area. It was idealized that the fin and wall (primary surface) have the same thermal conductivity and the surface heat transfer coefficient is uniform and equal on all surfaces. The temperature at the fin base was presented and compared with the temperature of the exposed wall surface in absence of the fin. They demonstrated the existence of the temperature depression by the presence of the fin and the results were presented for $mH = 1$ ($mH = K\text{Bi}^{1/2}$) and $\eta_i = 76.2$ percent. They found that for Bi = 0.25, 0.04, 0.01, and 0.0025 (correspondingly $K = 2$, 5, 10, and 20, respectively), the dimensionless temperature at the fin base θ_d is 77, 79, 85, 90 percent compared with the temperature of the exposed wall surface in the absence of fin. Here $\theta_d = (t_0 - t_a)/(t_s - t_a)$ and t_s is the temperature of the exposed wall surface in absence of the fin. The dimensionless temperature depression is then $1 - \theta_d$.

Klett and McCulloch (1972) analyzed a similar problem by using the same solution procedure as that in Sparrow and Hennecke (1970), but employing a different thermal conductivity of the fin material from that of the parent body (wall). The temperature depression at the fin base was presented for $mH = 1$, where m was based on the wall thermal conductivity. When the wall material was the same as the fin material, they reproduced Sparrow and Hennecke's (1970) results. For the fin material different from the wall material, they concluded that increasing the thermal conductivity of fin material decreases the temperature at the base, as one would expect. However, the results shown in their figures reveal the opposite conclusion. We believe the figures have typographical errors. The corrected results (presently calculated) are shown in Table 8, where $r_k = k_f/k_w$, $\text{Bi}_w = h\,\delta_f/k_w$.

Table 8 depicts two features: (1) for a given r_k and η_i, the temperature depression at the fin base increases (i.e., θ_d decreases) with increasing Bi_w (i.e., increasing h and δ_f), and (2) for given Bi_w and K, the temperature depression at the fin base increases with r_k or η_i.

Further studies of the temperature depression in multifin arrays were conducted by Sparrow and Lee (1975) for the straight fins of rectangular profile attached to a circular tube, and by Suryanarayana (1977) for straight fins attached to a plain wall. Both studies have taken into account the effects of the heat transfer coefficient on the back side of the finned wall (the other fluid side) and the presence and proximity of adjacent fins in the multifin array. Sparrow and Lee (1975) obtained a 2-D solution by solving the appropriate energy equations for the fin and the wall separately using a separation of variables method. From such a solution, uniform but different temperatures at the fin base and wall surface (primary surface) were obtained by averaging the temperature at the fin base and on the unfinned portion of the tube surface, respectively. These two uniform but different temperatures at the fin base and the unfinned base (tube area) were then used to calculate the fin heat flux and the heat flux on the unfinned base. The conventional analysis of heat transfer through a finned tube was employed as 1-D solution and assumed the outside surface temperature to be circumferentially uniform (Kern and Kraus 1972). This solution was found from an overall heat balance, which is based on purely radial heat conduction in the tube wall. The results showed that the 1-D solution overestimates the fin heat flux, but underestimates the heat flux on the unfinned base. They concluded that the fin heat flux error increases with an increase in the fin spacing, the heat flux error on the unfinned base increases with a decrease in the fin spacing, and the total heat transfer through the complete assembly could be higher or lower than that based on no temperature depression at the base.

Table 8 The dimensionless temperature at the fin base as a function of the ratio of thermal conductivity of the fin material to that of the wall material

r_k	Bi_w	K	η_i	θ_d percent
1	0.25	2	0.762	77.0
1	0.0625	4	0.762	78.0
1	0.0156	8	0.762	85.0
4	0.25	2	0.924	63.0
4	0.0625	4	0.924	70.0
4	0.0156	8	0.924	80.0
10	0.25	2	0.968	59.0
10	0.0625	4	0.968	68.0
10	0.0156	8	0.968	76.0
20	0.25	2	0.984	57.0
20	0.0625	4	0.984	66.5
20	0.0156	8	0.984	74.5

Suryanarayana (1977) presented multifin array numerical results for straight fins attached to a wall. He analyzed three 1-D models for the fin and the wall, and also one 2-D fin and wall assembly using a finite-difference technique. In his analysis, he covered the following ranges of parameters: Biot number of the fin based on the heat transfer coefficient on the fin surface as 0.1, the ratio of the heat transfer coefficient at the unfinned side to the finned side = 1, 10, 100, the ratio of the fin height to fin thickness = 1, 2.5, 5.0, the ratio of the fin spacing to fin thickness = 1.5, 2.0, 3.0, and the ratio of the wall thickness to fin thickness = 0.25, 0.5, 1, and 2.5. The nomenclature for a straight fin attached to a wall is shown in Figure 4. The first 1-D model assumed that the fin base (AB in Figure 4) temperature is the temperature of exposed wall surface in the absence of the fin. The second 1-D model ignored the thermal resistance of the wall (ABCD in Figure 4) and assumed that the fin base (AB in Figure 4) is directly exposed (without any thermal resistance) to the other side of the wall. The third 1-D model assumed that the wall (ABCD in Figure 4) is part of the fin, but only has y-direction heat transfer (assumed AC and BD in Figure 4 as insulated). He also analyzed the 2-D model of Figure 4 for the same range of parameters. Comparing with the 2-D solution, he concluded that the first and second 1-D models overestimate the fin heat flux, but the third 1-D model underestimates the fin heat flux. Unfortunately, he did not provide explicitly any results for the 2-D solution. Since none of his three 1-D models took into account the temperature depression effect, no conclusion on the effect of the temperature depression on the fin efficiency or total heat transfer can be derived from his results.

Heggs and Stones (1980) analyzed straight and annular fins numerically using a 2-D model considering finned and the unfinned regions of the extended surface exchanger as an entity (see Figure 4 for nomenclature for the straight fin). Note that Sparrow and Lee (1975) analyzed finned and unfinned regions separately. Heggs and Stones (1980) employed Equation 4 with $h_e = h$ for the 1-D fin analysis. Subsequently, they determined the total heat flow rate through the complete extended surface assembly, which includes both primary (unfinned) surface and the fins. For 1-D analysis, the total heat flow rate, q_1, through the complete extended surface assembly, was determined from

$$q_1 = (h_p A_p + \eta_i h_f A_f)\,\Delta T \tag{50}$$

where the subscripts p and f denote the primary and fin surfaces, respectively, ΔT is the temperature difference between

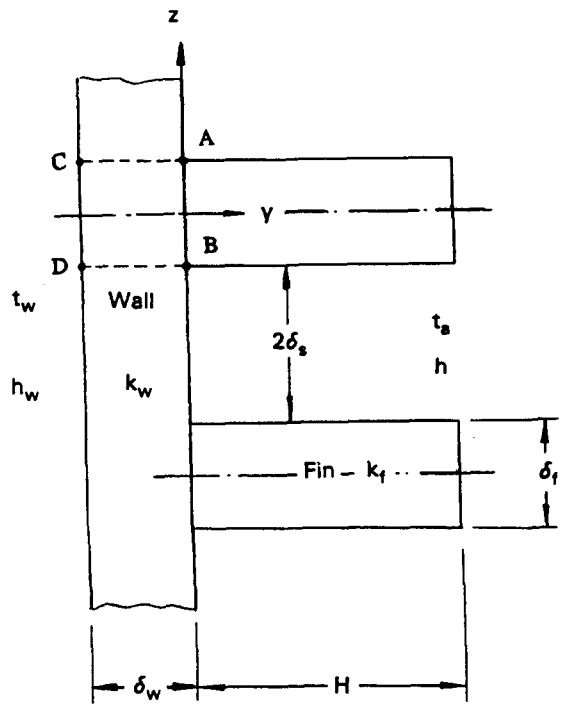

Figure 4 Nomenclature for longitudinal fin attached to a wall

the wall and ambient fluid, and η_i is given by Equation 4. In their analysis, they covered the following ranges of parameters: Biot number of the wall based on the unfinned (the other fluid) side heat transfer coefficient as 2, the ratio of the heat transfer coefficient at the unfinned side to finned side = 2–20,000, the ratio of the thermal conductivity of the fin to wall = 1–25, the ratio of the fin height to fin thickness = 1–160, the ratio of the fin spacing to fin thickness = 1–50, and the ratio of the wall thickness to fin thickness = 1–100. They found that the actual heat transfer rate through the extended surface assembly, using the more exact 2-D representation, is always higher than that from the 1-D model. The difference can be as high as about 20 percent, depending on the range of the parameters. However, for the industrially useful range of parameters ($Bi < 10^{-3}$ and $\eta_i > 80$ percent), the difference is about 4 percent or less. In contrast, it should be emphasized that Sparrow and Lee (1975) found that the effect of the fin base temperature depression is to increase or decrease the total heat transfer rate through the extended surface assembly; this is attributed to their different modeling and slightly different geometry.

Heggs *et al.* (1982) employed a series truncation method to study the 2-D straight fin problem considering finned and the unfinned regions of the extended surface exchanger as an entity. Manzoor (1984) conducted the same 2-D straight fin problem as that in Heggs *et al.* (1982) but employed finite-difference, finite-element, boundary integral equation, and series truncation methods. Both radiative and convective heat dissipation have been included in his model. He recommended that the boundary integral equation method be used for 2-D problems because it gives solutions of comparable accuracy to the finite-difference and finite-element methods, but is computationally more economical. He states that the series truncation method is by far the best suited to this particular problem because it gives the most accurate solutions with minimal computational requirements, if the problem does not involve curved or tapered fin profiles or nonuniform heat transfer coefficients. For 1-D analysis, Manzoor (1984) modified Equation 50 by including the radiation effect to calculate total heat flow rate through the complete extended surface assembly and Equation 4 for the 1-D fin. In his analysis, the results for two particular problems were presented: (1) $Bi = 10^{-5}$, $h_w/h = 200$, $k_f/k_w = 10$, $H/\delta_f = 100$, $\delta_s/\delta_f = 2$, $\delta_w/\delta_f = 1$, $\varepsilon_w = 0.6$, $\varepsilon_f = 0.8$, and the absolute temperature ratio, $t_w/t_a = 10$; and (2) $Bi = 2 \times 10^{-3}$, $h_w/h = 20$, $k_f/k_w = 20$, $H/\delta_f = 100$, $\delta_s/\delta_f = 2$, $\delta_w/\delta_f = 1$, $\varepsilon_w = 0.6$, $\varepsilon_f = 0.8$, and the absolute temperature ratio $t_w/t_a = 10$. He found that for problem 1 the heat transfer rate through the extended surface assembly using the 1-D model of Equations 4 and 50 is 2 percent lower than that from the more exact 2-D representation. This low 2 percent reduction is understandable since we found $\eta_1 = 0.92$ (a high value) from Equation 4. For problem 2, he found that heat transfer rate from the 1-D model is 27 percent higher than that from the more exact 2-D representation. For this case, we can calculate $\eta_i = 0.20$ from Equation 4, which is quite low, resulting in a greater difference between the 1-D and 2-D solutions. In contrast, it should be emphasized that Heggs and Stones (1980) found that the effect of the fin base temperature depression is only to increase the total heat transfer rate through the extended surface assembly. This may be attributed to their different modeling and without radiation heat transfer on the wall and fin surfaces.

Look (1989) analyzed the 2-D straight fin of rectangular profile with cosine fin base temperature to account for the effect of the fin base temperature depression. He employed heat balance integral approaches to solve Equation 9. Although no specific results are presented, he concluded that when $Bi \ll 1$, the effect of nonuniform fin base temperature is negligible.

Conclusions

The objective of this paper was to assess the accuracy of the conventional 1-D fin efficiency formula when the following usually neglected effects are included in the analysis: the effect of 2-D heat flow (thick fin), temperature dependent fin thermal conductivity, nonuniform heat transfer coefficient over the fin surface, nonuniform temperature of the ambient fluid, finite longitudinal heat conduction in the fin in the fluid flow direction, and temperature depression at the fin base. The following are specific conclusions:

(1) The ideal 1-D fin efficiency of Equation 5 is accurate to within 0.3 percent when compared with the exact 2-D expression of Equation 14 with $Bi^* = 0$ for $\eta_i > 80$ percent. When Bi is the order of 1 or less ($\eta_i < 80$ percent), the modified 1-D fin efficiency of Equation 21 with $Bi^* = 0$ has a less than 1 percent error compared with the exact 2-D expression of Equation 14 and is recommended over Equation 5.

(2) Considering a linear variation of the fin thermal conductivity up to 10 percent, the actual fin efficiency could be higher or lower compared with that by Equation 5 depending on whether the fin is being cooled or heated. However, the difference is within 2 percent for $\eta_i > 80$ percent. For a composite fin, the low conductivity layer plays a dominant role in the heat transfer mechanism; the reduction of heat flow by the so-called insulating layer due to frosting can be significant, about 8 percent at a typical η_i of 96 percent.

(3) The idealization of uniform heat transfer coefficient may lead to gross errors in analyzing extended surface heat transfer. For a particular linear variation of Equation 25, the actual fin efficiency will be lower by 6, 16, and 24 percent compared with that calculated from Equation 5 considering heat transfer coefficient, h_m, as constant for η_i of 90, 80, and 70 percent; here the mean value of the nonuniform heat transfer coefficient, h_m, is equal to the

value for the uniform case. In reality, since h for a given heat transfer surface is determined experimentally based on η_i for constant h, the idealization of constant h for determining η_i for the design of the exchanger would not introduce a significant error in η_f, particularly for high η_i such as $\eta_i > 80$ percent. However, one needs to be aware of the impact of nonuniform h on η_f if the heat exchanger test conditions and design conditions are significantly different.

(4) Nonuniform ambient temperature has less than a 1 percent effect on the fin efficiency for $\eta_i > 60$ percent and hence can be neglected.

(5) The longitudinal heat conduction effect on fin efficiency is less than 1 percent for $\eta_i > 10$ percent and hence can be neglected.

(6) The fin base temperature depression increases the total heat flow rate through the extended surface compared with that with no fin base temperature depression, and hence neglecting this effect provides a conservative approach for the extended surface heat transfer.

References

Anderson, D. A., Tannehill, J. C. and Pletcher, R. H. 1984. *Computational Fluid Mechanics and Heat Transfer*. Hemisphere, New York

Aparecido, J. B. and Cotta, R. M. 1990. Improved one-dimensional fin solutions. *Heat Trans. Eng.* **11**(1), 49–59

Avrami, M. and Little, J. B. 1942. Diffusion of heat through a rectangular bar and the cooling and insulating effects of fins. I. The steady state. *J. Applied Phys.* **13**, 255–259

Aziz, A. 1977. Perturbation solution for convective fin with internal heat generation and temperature-dependent thermal conductivity. *Int. J. Heat Mass Transfer* **20**, 1253–1255

Aziz, A. and Enamul Huq, S. M. 1975. Perturbation solution for convective fin with variable thermal conductivity. *J. Heat Transfer* **97**, 300–301

Barrow, H. 1985. A note on frosting of heat pump evaporator surface. *Heat Recovery Systems* **5**(3), 195–201

Barrow, H., Mistry, J. and Clayton, D. 1986. Numerical and exact mathematical analyses of two-dimensional rectangular composite fins. *Heat Transfer 1986*, **2**, 367–372

Chen, S. Y. and Zyskowski, G. L. 1963. Steady-state heat conduction in a straight fin with variable film coefficient. *ASME* Paper 63-HT-12

Cumo, M., Lopez, S. and Pinchera, G. C. 1965. Numerical calculation of extended surface efficiency. *Chem. Engrg. Prog. Symp. Series 59* **61**, 225–232

Epstein, N. and Sandhu, K. 1978. Effect of uniform fouling deposit on total efficiency of extended heat transfer surfaces. *Heat Transfer 1978*, **4**, 397–402

Fortescue, P. 1957. Some characteristics of reactor gas cooling systems. *Nucl. Power* **2**, 188–194

Ghai, M. L. 1951. Heat transfer in straight fins. *Proceedings of General Discussion on Heat Transfer*, Institution of Mech. Engineers, London, UK, 180–182, 203–204

Ghai, M. L. and Jakob, M. 1950. Local coefficients of heat transfer on fins. *ASME* Paper 50-5-18

Gardner, K. A. 1945. Efficiency of extended surface. *Trans. ASME* **67**, 621–631

Gardner, K. A. 1951. Discussion on paper of M. L. Ghai. *Proceedings of General Discussion on Heat Transfer*, Institution of Mech. Engineers, London, UK, 214–218

Han, L. S. and Lefkowitz, S. G. 1960. Constant cross-section fin efficiencies for nonuniform surface heat-transfer coefficients. *ASME* Paper 60-WA-41

Harris, M. J. and Wilson, J. T. 1961. Heat transfer and fluid flow investigation on large scale transverse fins. *Proc. of the Symp. on the Use of Secondary Surf. for Heat Transfer with Clean Gases*, Institution of Mech. Engineers, London, UK, 115–120

Heggs, P. J., Ingham, D. B. and Manzoor, M. 1982. The analysis of fin assembly heat transfer by a series truncation method. *J. Heat Transfer* **104**, 210–212

Heggs, P. J. and Stones, P. R. 1980. The effects of dimensions on the heat flowrate through extended surfaces. *J. Heat Transfer* **102**, 180–182

Hughes, D. F. and Slack, M. R. 1958. A correlation of heat transfer for finned fuel elements for carbon dioxide reactors. *Proc. 2nd United Nations Conf. on Peaceful Uses of Atomic Energy* **7**, 717–722

Hung, H. M. and Appl, F. C. 1967. Heat transfer of thin fins with temperature dependent thermal properties and internal heat generation. *J. Heat Transfer* **89**, 155–162

Irey, R. K. 1968. Errors in the one-dimensional fin solution. *J. Heat Transfer* **90**, 175–176

Jones, T. V. and Russell, C. M. B. 1978. Heat transfer distribution on annular fins. *AIAA-ASME Thermophysics and Heat Transfer Conf.*, Palo Alto, CA, USA

Jones, T. V. and Russell, C. M. B. 1980. Efficiency of rectangular fins. *ASME* Paper 80-HT-121

Keller, H. H. and Somers, E. V. 1959. Heat transfer from an annular fin of constant thickness. *J. Heat Transfer* **81**, 151–156

Kern, D. and Kraus, A. D. 1972. *Extended Surface Heat Transfer*. McGraw-Hill, New York

Klett, D. E. and McCulloch, J. W. 1972. The effect of thermal conductivity and base-temperature depression on fin effectiveness. *J. Heat Transfer* **94**, 333–334

Kraus, A. D. 1982. *Analysis and Evaluation of Extended Surface Thermal Systems*. Hemisphere, New York

Kraus, A. D., Snider, A. D. and Doly, L. F. 1978. An efficient algorithm for evaluating average of extended surface. *J. Heat Transfer* **100**, 288–293

Lau, W. and Tan, C. W. 1973. Errors in the one-dimensional heat transfer analysis in straight and annular fins. *J. Heat Transfer* **95**, 549–551

Look, Jr., D. C. 1988. Two-dimensional fin performance: Bi (top surface) $\geq$ Bi (bottom surface). *J. Heat Transfer* **110**, 780–782

Look, Jr., D. C. 1989. Two-dimensional fin with non-constant root temperature. *Int. J. Heat Mass Transfer* **32**, 977–980

Ma, S. W., Behbahani, A. I. and Tsuei, Y. G. 1991. Two-dimensional rectangular fin with variable heat transfer coefficient. *Int. J. Heat Mass Transfer* **34**, 79–85

Manzoor, M. 1984. Heat flow through extended surface heat exchangers. *Lecture Note in Engineering* (C. A. Brebbia, S. A. Orszag, Eds.), Springer-Verlag, New York

Mikhailov, M. D. and Özişik, M. N. 1984. *Unified Analysis and Solutions of Heat and Mass Diffusion*. John Wiley, New York

Özişik, M. N. 1985. *Heat Transfer—A Basic Approach*. McGraw-Hill, New York

Saboya, F. E. M. and Sparrow, E. M. 1976. Experiments on a three-row fin and tube heat exchanger. *J. Heat Transfer* **98**, 520–522

Schenck, H. 1960. *Heat Transfer Engineering*. Longman, White Plains, NY

Shah, R. K. 1971. Temperature effectiveness of multiple sandwich rectangular plate-fin surface. *J. Heat Transfer* **93**, 471–473

Shah, R. K. 1985. Compact heat exchangers. *Handbook of Heat Transfer Applications* (W. M. Rohsenow, J. P. Hartnett and E. N. Ganić, Eds.). McGraw-Hill, New York, 174–312

Snider, A. D. and Kraus, A. D. 1982. Correcting for the variability of the heat transfer coefficient in extended surface analysis. *Heat Transfer 1982*, **6**, 239–243

Sparrow, E. M. and Hennecke, D. K. 1970. Temperature depression at the base of a fin. *J. Heat Transfer* **92**, 204–206

Sparrow, E. M. and Lee, L. 1975. Effects of fin base-temperature depression in a multifin array. *J. Heat Transfer* **97**, 463–465

Stachiewicz, J. W. and McKay, A. R. 1963. Heat transfer coefficients on finned surfaces. *Trans. EIC* **1**, B-9

Steir, A. A. 1976. The heat balance integral in steady-state conduction. *J. Heat Transfer* **98**, 466–470

Stynes, S. K. and Myers, J. E. 1964. Transport from extended surfaces. *AIChE J.* **10**, 437–442

Suryanarayana, N. V. 1977. Two-dimensional effects on heat transfer rates from an array of straight fins. *J. Heat Transfer* **99**, 129–132

Ünal, H. C. 1985. Determination of the temperature distribution in an extended surface with a non-uniform heat transfer coefficient. *Int. J. Heat Mass Transfer* **28**, 2279–2284

Ünal, H. C. 1987. Temperature distributions in fins with uniform and non-uniform heat generation and non-uniform heat transfer coefficient. *Int. J. Heat Mass Transfer* **30**, 1465–1477